Lawrence Berkeley National Laboratory
Recent Work

Title

Protein-protein and Protein-solved Interactions in Aqueous Protein Solutions Containing Concentrated Electrolytes

Permalink

https://escholarship.org/uc/item/5wq2r9ng

Author

Curtis, R.A.

Publication Date

1996-10-01

eScholarship.org Powered by the California Digital Library
University of California

LBNL-39460
UC-401
Preprint

ERNEST ORLANDO LAWRENCE
BERKELEY NATIONAL LABORATORY

Protein-Protein and Protein-Salt Interactions in Aqueous Protein Solutions Containing Concentrated Electrolytes

R.A. Curtis, H.W. Blanch, and J.M. Prausnitz
Chemical Sciences Division

October 1996
Submitted to
Biotechnology and Bioengineering

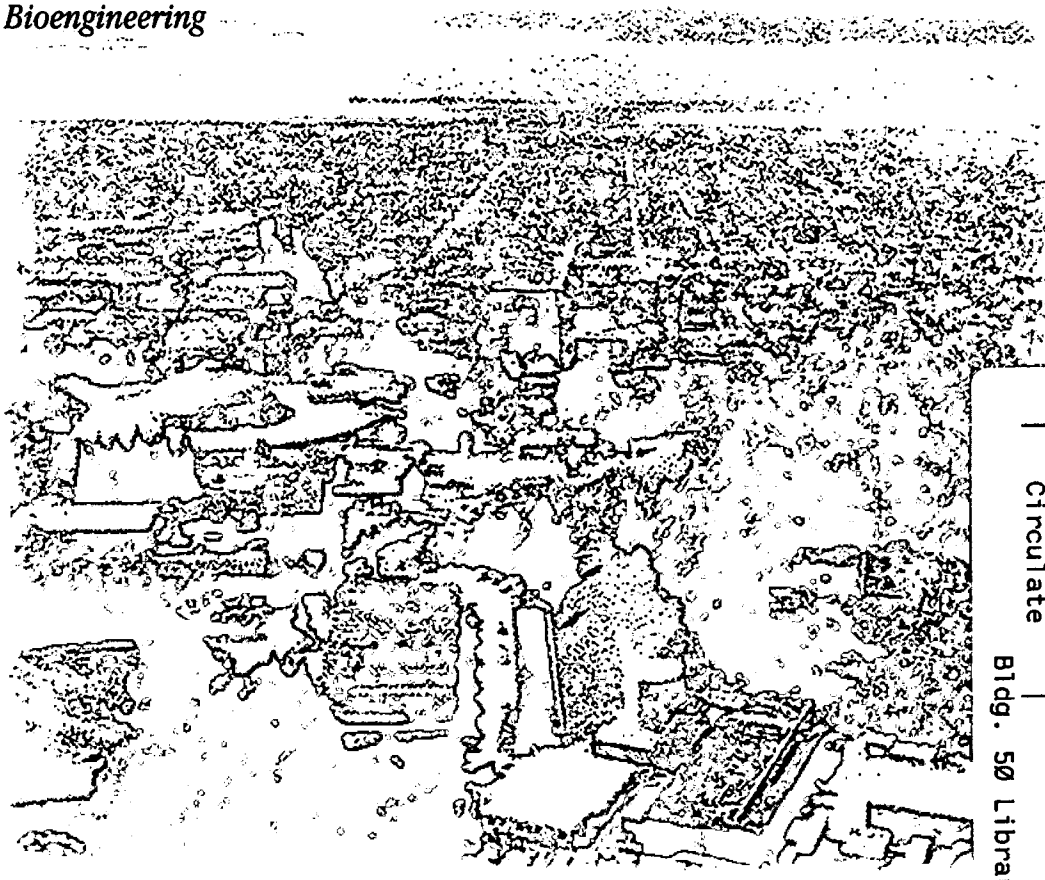

REFERENCE COPY
Does Not
Circulate
Bldg. 50 Library.
Copy 1
LBNL-39460

DISCLAIMER

This document was prepared as an account of work sponsored by the United States Government. While this document is believed to contain correct information, neither the United States Government nor any agency thereof, nor the Regents of the University of California, nor any of their employees, makes any warranty, express or implied, or assumes any legal responsibility for the accuracy, completeness, or usefulness of any information, apparatus, product, or process disclosed, or represents that its use would not infringe privately owned rights. Reference herein to any specific commercial product, process, or service by its trade name, trademark, manufacturer, or otherwise, does not necessarily constitute or imply its endorsement, recommendation, or favoring by the United States Government or any agency thereof, or the Regents of the University of California. The views and opinions of authors expressed herein do not necessarily state or reflect those of the United States Government or any agency thereof or the Regents of the University of California.

LBNL-39460
UC-401

Protein-Protein and Protein-Salt Interactions in Aqueous Protein Solutions Containing Concentrated Electrolytes

R. A. Curtis and *H. W. Blanch

Department of Chemical Engineering

University of California

and

J. M. Prausnitz

Dept. of Chemical Engineering

University of California

and

Chemical Sciences Division, Lawrence Berkeley National Laboratory

University of California

Berkeley, CA 94720, U.S.A.

*Corresponding author

Key Words:

Proteins, Salts, Intermolecular Interactions, Potentials of Mean Force,

Precipitation, Crystallization

This work was supported by the Director, Office of Energy Research, Office of Basic Energy Sciences, Chemical Sciences Division of the U.S. Department of Energy under Contract Number DE-AC03-76SF00098.

Introduction

Recovery and purification of proteins is an area of major importance in biotechnology. Recombinant therapeutic proteins have current sales of over $5 billion; they include blood products, hormones (e.g., erythropoietin, insulin), growth factors, cytokines (e.g., interferons and interleukins), and monoclonal antibodies. Separation and purification processes for these products are governed by interactions of proteins with themselves, salts, charged and hydrophobic surfaces, or added solutes such as polymers or organic solutes. The types of interactions and their importance in protein separation processes are shown below.

Type of interaction	*Example of separation processes where the interaction is important*
Electrostatic (e.g., charge-charge)	ion exchange, electrodialysis, electrophoresis
Hydrophobic and dispersion	hydrophobic interaction chromatography
Steric (excluded volume)	precipitation by salts and by polymers
Interaction with external field	gel filtration, centrifugation, electrophoresis
Specific chemical (e.g. epitope specific)	affinity chromatography, precipitation

At fixed conditions, the magnitude of these interactions is determined by protein structure. Key parameters are protein size and shape, surface charge, presence of apolar surface residues, and amino-acid residues that participate in specific interactions (e.g., ligand-receptor, antigen-antibody).

Intermolecular interactions are also important in understanding biochemical reactions within the cell. The rate of physiological processes is dependent on steric interactions which are determined from the extent of macromolecular crowding (Zimmerman and Minton, 1993). The stability of protein drugs formulated with stabilizing agents also depends on steric and electrostatic interactions. For example, insulin frosting on the walls of insulin containers is a problem associated with loading insulin into long-term infusion devices. Protein precipitation is a sympton, or possibly a cause, in Alzheimer's disease, cataract formation, Down's syndrome and crush injury.

Salt-induced protein precipitation is an extensively used method as an initial step to purify proteins because of its low cost and selectivity. For example, protein precipitation has been used industrially to separate proteins from blood plasma (Stryker et al., 1985), from bacterial extracts (Lambert and Meers, 1983), and from plant extracts (Jervis and Pierpoint, 1989). Protein precipitation has been the subject of several extensive reviews, including those of Foster (1994) and Rothstein (1994). The solubilites of proteins in aqueous electrolyte solutions are determined by the magnitude of protein-protein and protein-salt interactions.

Chiew et al. (1995) have illustrated the importance of excluded-volume, hydrophobic, and specific interactions between proteins in the partitioning of proteins between a dilute liquid and an amorphous precipitate phase. The importance of protein-protein interactions in protein crystallization has been demonstrated by George and Wilson (1994). These authors have proposed that a crystallization "window" exists for the protein-protein second virial coefficient, B_{22}, which is a direct measure of the protein-protein pair potential. As a necessary condition for protein crystallization, B_{22} should be in the region $-2x10^{-4}$ mLmol/g^2 and $-8x10^{-4}$ mLmol/g^2. For B_{22} more positive than $-2x10^{-4}$ mLmol/g^2, the protein-protein attraction is not strong enough to form stable protein crystals. For solutions where the magnitudes of B_{22} are greater than $-8x10^{-4}$ mLmol/g^2, amorphous precipitation occurs because the protein-protein attractions are sufficiently strong that the protein molecules do not have sufficient time to orient themselves to form crystals before forming an amorphous second phase.

The importance of protein-salt interactions in determining protein solubility has been stressed by Melander and Horvath (1977) and Arakawa et al. (1985, 1990). In general, the effect of salt on protein solubility can be described by a salting-in region at low salt concentrations and a salting-out region for high ionic-strength solutions. The salting-in region is a result of favorable electrostatic interactions between the salt ions and the charged residues of the protein. At higher salt concentrations, most salt ions are

excluded from the protein's domain due to unfavorable interactions between the salt ions and the hydrophobic residues, which results in salting-out behavior. However, Timasheff and Arakawa (1990) have shown negatively-charged proteins are solubilized at high salt concentrations in the presence of divalent cations. This behavior is attributed to specific binding of the divalent cation to the protein.

Salts are also important for protein crystallization. They can behave as either protein-structure stabilizers or co-crystallization agents (McPherson, 1990; Lovrien et al., 1996). To form good-quality crystals, the protein molecules should be structurally homogeneous which implies that their native forms have high conformational stability. Kosmotropic salts (high lyotropic-series salts), such as the sulfate and acetate ions, tend to stabilize the native state of the protein by strengthening the hydrophobic interactions between apolar residues which are exposed during protein unfolding. Some salts co-crystallize with proteins and increase crystal stability by reducing the crystal-phase electrostatic free energy. Examples include SCN^- and lysozyme crystals (Howell et al., 1995) and PO_4^{-2} and insulin crystals (Takahashi, 1993). In most cases, however, salts with the highest binding affinities are chaotropic salts (low lyotropic-series salts), such as SCN^- and NO_3^-.

In this paper we describe and present data for the important protein-protein and protein-salt interactions that are responsible for salt-induced precipitation of proteins. Our discussion also concerns the relationship of intermolecular interactions to protein solubility and to the implications for crystallization versus amorphous precipitation.

Protein-Salt Interactions

Protein-salt interactions can be measured by a variety of techniques including densimetry, differential refractometry, and vapor-pressure equilibrium (Lee, Gekko, and Timasheff, 1977). All of these measurements yield a preferential-interaction parameter, a quantity that reflects the interaction between the salt and the macromolecule. This

parameter is a measure of the difference in solvent composition around the protein relative to that in the bulk solution. In this sense, it can be thought of as the excess (or deficiency) of the salt per protein molecule inside a dialysis bag relative to the salt concentration outside the dialysis bag.

For the water (1), protein (2), and salt (3) system, the preferential-interaction parameter, $(\partial m_3/\partial m_2)_{T,P,\mu_3}$ is approximately equal to the experimentally-determinable parameter $(\partial m_3/\partial m_2)_{T,\mu(d)}$ at infinite dilution of protein.

$$\left(\frac{\partial m_3}{\partial m_2}\right)^{\infty}_{T,\mu(d)} \approx \left(\frac{\partial m_3}{\partial m_2}\right)^{\infty}_{T,P,m} \qquad (1)$$

where m_i is the molality of component i, μ_i is the chemical potential of component i, and superscript ∞ indicates that the quantity is at infinite dilution of the protein. $\mu(d)$ represents the set of chemical potentials of the solvent components (i.e. salt and water) and the subscript m signifies that all the molalities, except the one indicated by the differentiation, are constant. $(\partial m_3/\partial m_2)_{T,\mu(d)}$ can be determined from refractive-index increments. For the three-component system, the change in refractive-index, n, in terms of molalities, is given by

$$dn = \left(\frac{\partial n}{\partial m_2}\right)_{T,P,m} dm_2 + \left(\frac{\partial n}{\partial m_3}\right)_{T,P,m} dm_3 \qquad (2)$$

Taking the derivative of Equation 2 with respect to the protein molality at constant solvent chemical potential and temperature, gives

$$\left(\frac{\partial m_3}{\partial m_2}\right)^{\infty}_{T,\mu(d)} = \frac{(\partial n/\partial m_2)^{\infty}_{T,\mu(d)} - (\partial n/\partial m_2)^{\infty}_{T,P,m}}{(\partial n/\partial m_3)_{T,P,m}} \qquad (3)$$

Since the refractive-index increments are most easily measured in terms of weight concentrations, Equation 3 is converted to the following expression (Inoue and Timasheff, 1968; Casassa and Eisenberg, 1964):

$$\left(\frac{\partial m_3}{\partial m_2}\right)^{\infty}_{T,\mu(d)} = \frac{M_2}{M_3(1-\bar{v}_3 c_3)} \frac{\left[(\partial n/\partial c_2)^{\infty}_{T,\mu(d)} - (\partial n/\partial c_2)^{\infty}_{T,P,m}\right]}{(\partial n/\partial c_3)_{T,P,m}} \qquad (4)$$

where c is in units of weight concentration, $(\partial n/\partial c_3)_{T,m}$ is the refractive-index increment of the salt and $\bar{v}_3$ is its partial specific volume.

The difference between $(\partial n/\partial c_2)^{\infty}_{T,\mu(d)}$ and $(\partial n/\partial c_2)^{\infty}_{T,P,m}$ is due to the unequal concentrations of the salt across a dialysis membrane, when the chemical potential of the salt is the same on both sides of the membrane. In the ideal case, where the activity of the salt is not perturbed by the presence of the protein, there is no driving force for unequal distribution of the salt and $(\partial n/\partial c_2)^{\infty}_{T,\mu(d)}$ and $(\partial n/\partial c_2)^{\infty}_{T,P,m}$ are equal. The amount that the salt redistributes across a dialysis membrane increases with salt concentration, due to the law of mass action. Thus, at low salt concentrations, differential refractometry is not an accurate method for determining preferential-interaction parameters because the refractive-index increment measurements are not sufficiently sensitive to detect the small difference in salt concentrations across the membrane.

The preferential-interaction parameter is equal to the perturbation of the salt activity by the addition of the protein (Timasheff and Arakawa, 1985, 1988; Lee, Gekko, and Timasheff, 1979)

$$\left(\frac{\partial m_3}{\partial m_2}\right)_{T,P,\mu_3} = -\frac{(\partial \mu_2/\partial m_3)_{T,P,m}}{(\partial \mu_3/\partial m_3)_{T,P,m}} \qquad (5)$$

μ_2 and μ_3 are the chemical potentials of the protein and the salt. $(\partial\mu_3/\partial m_3)_{T,P,m}$ can be calculated from activity-coefficient data of the aqueous salt solutions.

The quantity $(\partial\mu_2/\partial m_3)_{T,P,m}$ can be calculated from expressions for the Gibbs energy required to transfer a protein from salt-free water solution to the salt solution, $\Delta\mu_2^1$, both at infinite dilution of protein. Melander and Horvath have calculated $\Delta\mu_2^1$ using expressions of Debye-Hückel (Tanford, 1961) and Kirkwood (1943) for the interaction between the charge and dipole moment of the protein with the salt ions and the expression from Sinanoglu cavity theory (1968) for hydrophobic interactions. Arakawa, Bhat, and Timasheff (1990) have further modified this equation by including an additional term to account for specific binding of salt ions to the protein. The resulting expression for $\Delta\mu_2^1$ is

$$\Delta\mu_2^1 = -\frac{A_{z_2} I^{1/2}}{1 + B_{z_2} I^{1/2}} + A_\sigma m_3 - A_\mu I - f_{bind}(k_{bind} m_3, Z_2) \qquad (6)$$

where I is the ionic-strength. A_{z_2} and B_{z_2} are constants derived from Debye-Hückel theory (Tanford, 1961), which account for the decrease in Gibbs energy of the protein due to favorable electrostatic interactions between the charged residues of the protein and oppositely charged salt ions. Kirkwood (1943) has developed an expression for the decrease in Gibbs energy as a result of the interaction between the protein dipole and the salt ions, given by A_μ. A_σ is related to the Gibbs energy required to form a cavity in the solvent as given by Sinanoglu (1968). This term is usually positive since most inorganic salts raise the surface tension of water. The ion-binding contribution has been estimated by Tanford (1961) by assuming weak ion binding at identical sites. The result is $f_{bind} = nRT\ln\left[1\Big/\left(1 + k_{bind} m_3 e^{-\Gamma(Z_2)}\right)\right]$ where n is the number of binding sites, k_{bind} is the equilibrium constant for the binding, and $\Gamma(Z_2)$ is the electrostatic work term that accounts for the effect of the charge of the protein on k_{bind}. Figure 1 shows $\Delta\mu_2^1$ as a

function of salt molality (m_3). Arakawa et al. (1982, 1988, 1990) have shown good agreement between calculated and experimental values of $\Delta\mu_2^1$ for systems which do or do not exhibit specific ion binding. Experimental values of $\Delta\mu_2^1$ are obtained by integration of the preferential-interaction parameter according to

$$\Delta\mu_2^1 = \int_0^{m_3} (\partial\mu_2/\partial m_3)_{m_2} dm_3 = -\int_0^{m_3} (\partial\mu_3/\partial m_3)_{m_2} (\partial m_3/\partial m_2)_{\mu(d)} dm_3 \qquad (7)$$

Negative values of $\Delta\mu_2^1$ are unfavorable and lead to salting-out. Figure 1 shows that the solubility at high salt concentrations is determined from unfavorable interactions due to the increase in surface tension of the solvent, and that the salting-in effect is due to weak ion binding.

Protein-Protein Interactions

Protein-protein interactions can be probed by a variety of techniques including membrane osmometry, sedimentation, and low-angle laser-light scattering (LALLS). All of these techniques yield a protein-protein osmotic second virial coefficient (B_{22}) which can be related to the sum of the potentials-of-mean-force. The potential-of-mean-force is defined such that its negative derivative with respect to distance is the force between two solute molecules at infinite dilution, averaged over all configurations of the solvent molecules (McMillan and Mayer, 1945). If the sum of the potentials-of-mean-force (W_{22}) is spherically symmetric (Hill, 1957), B_{22} is given by the following volume integral:

$$B_{22}(\mu(d)^o, T) = -\frac{N_A}{2} \int_0^{\infty} \left[\exp\left(-W_{22}(r, \mu(d)^o, T)/kT\right) - 1\right] 4\pi r^2 dr \qquad (8)$$

where $\mu(d)^o$ represents the set of chemical potentials of solvent components at zero protein concentration, T is temperature, N_A is Avogadro's number, k is Boltzmann's constant, and r is the center-to-center separation of the two solute molecules.

For globular (essentialy spherical) proteins in moderate to high ionic-strength salt solutions, an adequate model for W_{22} is given by the sum of the following spherically symmetric potentials:

$$W_{22}(r) = W_{hs}(r) + W_{disp}(r) + W_{elec}(r) + W_{osmotic}(r) \qquad (9)$$

where r is the center-to-center distance. Here, $W_{hs}(r)$ is the protein hard-sphere (excluded-volume) potential, $W_{disp}(r)$ is the dispersion potential of Hamaker, $W_{elec}(r)$ is the repulsive coulombic potential due to charge on the protein, and $W_{osmotic}(r)$ is an attractive interaction due to the excluded-volume effect of the salt ions. The first three terms, $W_{hs}(r)$, $W_{disp}(r)$, and $W_{elec}(r)$, are described by DLVO theory (Verwey and Overbeek, 1948) where proteins are modeled as rigid spheres with uniform surface charge immersed in a continuous dielectric medium containing point charges depicting salt ions. Osmotic pressures for proteins at low salt concentrations may be predicted accurately by the DLVO model (Vlachy and Prausnitz, 1992; Vilker et al., 1981). However, at higher salt concentrations, the excluded volume of the salt ions is significant and $W_{osmotic}(r)$ must be included in the model (Vlachy and Prausnitz, 1992; Vlachy et al., 1993). Higher-order electrostatic interactions, including dipole-charge and dipole-dipole interactions have been typically omitted because they are effectively screened out at the high experimental salt concentrations employed. However, at low ionic strengths, Coen et al. (1995) have shown that B_{22} becomes significantly more negative because of higher-order electrostatic interactions.

The excluded volume of the protein is accounted for by the hard-sphere potential (Verwey and Overbeek, 1948):

$$W_{hs(r)} = \infty \qquad \text{for} \qquad r \le d_2 + 2\sigma \tag{10}$$

where d_2 is the protein diameter and σ is the thickness of a water layer bound to the protein.

The screened coulombic repulsion potential between two proteins is derived from Debye-Hückel theory (Verwey and Overbeek, 1948):

$$\frac{W_{elec}(r)}{kT} = \frac{z^2e^2(1/r)\exp[-\kappa(r-d_2]}{4\pi kT\varepsilon_o\varepsilon_r(1+d_2/2)^2} \qquad \text{for} \quad r > d_2 + 2\sigma \tag{11}$$

where ze is the charge of the protein, $4\pi\varepsilon_o$ is the dielectric permittivity of free space in SI units (C/Jm), d_2 is the hard-sphere diameter, ε_r is the relative dielectric permittivity of water. κ is the inverse of the Debye length given by $\kappa^2=(2e^2N_AI)/(kT\varepsilon_o\varepsilon_r)$, where N_A is Avogadro's number, I is the ionic strength of the salt, and e is unit charge. The approximation that the salt ions behave as point charges is poor at ionic strengths greater than 0.1 molar. However, because at these salt concentrations the coulombic repulsion between protein molecules is effectively screened out, this assumption is of no significance when calculating the electrostatic contribution to B_{22}.

The attractive Hamaker dispersion interaction is given by (Hamaker, 1937):

$$\frac{W_{disp}(r)}{kT} = -\frac{H}{12}\left\{\frac{d_2^2}{r^2-d_2^2} + \frac{d_2^2}{r^2} + 2\ln\left(1-\frac{d_2^2}{r^2}\right)\right\} \qquad \text{for} \quad r > d_2 + 2\sigma \tag{12}$$

where H is the effective Hamaker constant for the protein-protein interaction. Hamaker constants depend on the composition and on the density of the protein and on the chemical nature of the solute (Nir, 1976). The dispersion interaction is independent of ionic strength because the correlation time of the electronic fluctuations between atoms is much smaller than the time for adjustment of ions in the double layer (Israelachvili,

1992). However, the Hamaker constant may depend on pH as a result of possible pH-induced protein conformational changes. In general, because different proteins have similar densities and compositions, they also have similar Hamaker constants. A good approximation for the Hamaker constant of a protein is on the order of 5 kT (Nir, 1976).

At higher electrolye concentrations, the excluded volume of the ions is important. A possible potential for this interaction is the osmotic-attraction potential of Asakura and Oosawa (1954, 1958):

$$\frac{W_{osmotic}(r)}{kT} = -\frac{4}{3}\pi\sigma^3(\rho_s kT)\left[1 - \frac{3r}{4d_{23}} + \frac{r^3}{16d_{23}^3}\right] \qquad (13)$$

$$d_{23} = (d_2 + d_3 + 2\sigma)/2 \qquad \text{for} \qquad d_2 + 2\sigma < r < d_2 + 2\sigma + d_3$$

where d_3 is the mean ionic diameter and ρ_s is the total ion concentration. When two proteins are near contact, the salt ions are excluded between them giving rise to an imbalance of pressure around the proteins due to the differences in local concentrations of salt ions. Equation (13) is derived by approximating this osmotic-pressure difference by the ideal osmotic pressure ($\Pi_{id}=\rho_s/kT$) of the salt solution.

In addition, when salt is excluded between proteins, specific short-range electrostatic interactions, such as hydrogen bonds and salt bridges, may be important. These types of interactions have been shown to stabilize protein crystals; they may also be significant in solution as suggested by Wilson (1996) who showed that experimentally-determined changes in B_{22} with temperature paralleled changes in protein solubility. Since the protein solubility is a direct measure of the crystal chemical potential, this result implies that protein-protein interactions related to B_{22} for proteins in dilute solution can be extrapolated to protein-protein interactions in the crystal.

Theories Describing Protein Solubility

The solubility of a given solute in a solvent is determined by the net result of the solvent-solvent, solvent-solute, and solute-solute interactions. Statistical-mechanical theories that predict protein phase behavior employ integral-equation theory to calculate the pair distribution functions, $g_{ij}(r)$, between all types of solute molecules. $g_{ij}(r)$ is directly related to the pair potential of mean force, $W_{ij}(r)$ by

$$g_{ij}(r) = \exp(-W_{ij}(r)) \tag{14}$$

Perturbation theories can then be used to calculate the excess energies and chemical potentials of the system from $W_{ij}(r)$. The phase behavior follows from the condition that the chemical potential of a solute is the same in both phases.

At the present time, there are only a few theories for predicting phase separation for solutions of protein and concentrated electrolyte. Rosenbaum et al. (1996) have shown that lysozyme molecules can be modeled as adhesive hard spheres, dispersed in a pseudo-solvent of salt and water. Their experimental results for the crystal-liquid phase separation of lysozyme in concentrated salt solution are in qualitative agreement with theoretical predictions where the protein-protein potential-of-mean-force is given by Baxter's adhesive hard-sphere potential (Baxter, 1968). These authors propose that a short-ranged potential provides an accurate means for predicting the phase behavior since all protein interactions have very short ranges at ionic strengths greater than 0.1 molar. Chiew et al. (1995) modeled the liquid-liquid phase separation of proteins in a concentrated salt solution using a potential-of-mean-force describing the protein-protein interaction. Hard-sphere, electrostatic, dispersion, ion-excluded-volume, and hydrophobic potentials are included in the model. A result of this model is that the protein phase behavior is independent of protein net charge (i.e. pH) since the model contains no pH-dependent protein-protein interactions at high salt concentrations. To

improve this model, either a pH dependent interaction needs to be considered, such as short-range electrostatic interactions discussed in the *Protein-Protein Interactions* Section, or the salt needs to be modeled explicitly, accounting for short-range electrostatic interactions between the protein and the salt. A successful model must include the observed pH dependence of solubility at high ionic strength.

A different approach for predicting protein solubility in concentrated aqueous electrolyte solutions has been provided by Melander and Horvath (1977) who give a theoretical interpretation of the salting-out equation of Cohn (1925) that is based on the expressions for the Gibbs energy of transfer, $\Delta\mu_2^l$. This approach has been expanded by Arakawa and Timasheff (1985, 1990) who have predicted experimentally-determinable preferential-interaction parameters between the protein and salt from expressions for the Gibbs transfer energies. Arakawa and Timasheff (1990) determined the dependence of protein solubility on the preferential-interaction parameters and thereby the Gibbs transfer energies according to Equation 7.

Protein solubility is determined from the chemical equilibrium condition between the liquid and the dense (i.e. amorphous precipitate or crystal) phase. At equilibrium, the chemical potential of the protein is the same in both phases.

$$\mu_2 = \mu_2^d + RT\ln a_2 = \mu_2^l + RT\ln\gamma_2 S_2 \qquad (15)$$

where μ_2^d and μ_2^l are the reference chemical potentials for the protein in the dense and liquid phases, respectively. The equilibrium solubility of the protein is S_2, while a_2 is the activity of the protein in the dense phase, and γ_2 is the activity coefficient of the dissolved protein. The reference chemical potential in the liquid phase, μ_2^l, is so chosen that the activity coefficient of the protein approaches unity as the protein concentration approaches zero. By this definition, μ_2^l only accounts for contributions from the protein-solvent interactions to the protein chemical potential, since the reference solution is the

ideal state in which the protein molecules are at infinite dilution in the solvent. The contributions from the protein-protein interactions to μ_2 are reflected in activity coefficient, γ_2. The separation of the protein-protein and protein-salt interactions in the dense phase can be performed by defining the reference state to be a hypothetical phase in which the protein-protein interactions are absent. With this definition, the protein activity, a_2, accounts for turning on the protein-protein interactions.

The empirical salting-out equation of Cohn (1925) can be interpreted by considering the difference between the protein solubility in aqueous salt solution and that in salt-free water. From Equation 15, the protein solubility in the salt solution with respect to its solubility in salt-free water is

$$\ln\left(\frac{S_{2,s}}{S_{2,w}}\right) = \ln\left(\frac{a_{2,s}}{a_{2,w}}\right) - \ln\left(\frac{\gamma_{2,s}}{\gamma_{2,w}}\right) + \frac{\Delta\mu_2^d}{RT} - \frac{\Delta\mu_2^l}{RT} \qquad (16)$$

where

$$\Delta\mu_2^d = \mu_{2,s}^d - \mu_{2,w}^d \qquad (17a) \qquad \Delta\mu_2^l = \mu_{2,s}^l - \mu_{2,w}^l \qquad (17b)$$

The subscripts, s and w, refer, respectively, to equilibrium conditions in the aqueous salt solution and in the salt-free solution. $\Delta\mu_2^d$ and $\Delta\mu_2^l$ represent the transfer Gibbs energies of the protein from salt-free water to salt solution in the dense and liquid phases.

However, Equation 16 can be misleading when considering equilibrium solubilities of amorphous precipitates because it has been shown that the concentration of the amorphous precipitate phase is a strong function of the salt concentration, pH, and, in particular, the initial protein concentration used in the experiment (Shih et al., 1992; Coen et al., 1996). Since initial protein concentration affects the protein concentration of the amorphous precipitate phase, a universal solubility does not exist for a given pH and salt concentration. For these cases, Equation 16 can be reformulated by replacing the activity

of the dense phase with an activity coefficient multiplied by the concentration of the dense phase.

$$\ln\left(\frac{c_{2,s}^{l}/c_{2,s}^{d}}{c_{2,w}^{l}/c_{2,w}^{d}}\right) = \ln\left(\frac{\gamma_{2,s}^{d}}{\gamma_{2,w}^{d}}\right) - \ln\left(\frac{\gamma_{2,s}^{l}}{\gamma_{2,w}^{l}}\right) + \frac{\Delta\mu_2^{d}}{RT} - \frac{\Delta\mu_2^{l}}{RT} \qquad (16a)$$

Here, the important quantity is the protein partition coefficient which is defined as the ratio of the concentration of the protein in the supernatant phase (c_2^l) to that in the dense phase (c_2^d).

The Cohn equation is given by

$$\ln S_{2,s} = \beta - K_s m_3 \qquad (18)$$

where $S_{2,s}$ is the solubility of the protein in an aqueous salt solution of molality m_3; K_s is the salting-out constant; and β represents a hypothetical solubility at zero molality. K_s, can be calculated from Equation 16

$$K_s = \left(\frac{\partial \ln S_{2,s}}{\partial m_3}\right)_T \qquad (19)$$

Melander and Horvath (1977) and Arakawa, Bhat, and Timasheff (1985, 1990) have shown that Equation 19 can be evaluated from the expressions given for the Gibbs transfer energies in Equation 6, neglecting the dependence of the activity coefficient and activity terms on the salt molality. However, the solubility of the protein can be a strong function of β which depends on the activities of the protein in the solid phases and the activity coefficients of the dissolved protein.

Protein-Protein Interactions Determined by Light-Scattering

Low-angle laser-light scattering (LALLS) is the principal method for determining weight-average molecular weights, osmotic second virial coefficients, and molecular dimensions in dilute macromolecular solutions. The generalized equation for the experimentally determinable Rayleigh ratio, R_θ, is given by (Stockmayer, 1950; Kirkwood and Goldberg, 1950)

$$R_\theta = R_\rho + KV_m RT \sum_j \sum_k \left(\partial n/\partial m_j\right)_{T,P,m} \left(\partial n/\partial m_k\right)_{T,P,m} / \left(\partial \mu_j/\partial m_k\right)_{T,P,\mu} \qquad (20)$$

where V_m is the volume of the solution in mL containing 1 kg of the principal solvent (i.e. component 1), n is the refractive index, and R is the universal gas constant. K is the light-scattering constant given by $2\pi^2 n^2/N_A\lambda^4$ where λ is the wavelength of the incident light and R_ρ is the scattering that arises from the density fluctuations of the solvent, given by

$$R_\rho = \kappa RT\left(\partial n/\partial p\right)_{T,m}/K \qquad (21)$$

where κ is the compressibility of the solvent. Subscripts m and μ signify constancy of all molalities and chemical potentials except the ones indicated by the differentiation.

For the three component system water (1), protein (2), and salt (3), Equation 20 reduces to

$$\frac{Kc_2\left(\partial n/\partial c_2\right)^2_{T,P,m}}{\overline{R_\theta}} = \frac{1}{\Omega^2}\left(\frac{1}{M_2} + \frac{2}{M_2^2}\left(B_{22} - \left(\frac{\partial m_3}{\partial m_2}\right)^{\infty}_{P,\mu(d)} \overline{V}_3^{\infty}\right)c_2\right) \qquad (22)$$

where

$$\Omega = 1 + \frac{\left(\partial n/\partial m_3\right)_{P,m}}{\left(\partial n/\partial m_2\right)_{P,m}}\left(\frac{\partial m_3}{\partial m_2}\right)_{P,\mu} \qquad (23)$$

$\overline{R_\theta}$ is the excess Rayleigh scattering of the protein solution over the aqueous salt solution ($R_\theta - R_\rho$) and $\overline{V}_3^\infty$ is the partial molar volume of the salt at infinite dilution of protein. If we substitute $(\partial n/\partial c_2)_{T,\mu(d)}$ for $(\partial n/\partial c_2)_{T,P,m}$, Equation 22 reduces to

$$\frac{Kc_2(\partial n/\partial c_2)_{T,\mu(d)}}{\overline{R_\theta}} = \frac{1}{M_2} + 2\frac{B_{22}}{M_2^2}c_2 \qquad (24)$$

Thus, if the refractive-index of the protein at constant chemical potential, $(\partial n/\partial c_2)_{T,P,\mu(d)}$, is known, B_{22} can be directly determined. If the protein exists solely as monomers in solution, a plot of $K(\partial n/\partial c_2)_{T,P,\mu(d)}c_2/\overline{R_\theta}$ versus c_2 can be used to determine the osmotic second virial coefficient, B_{22}, and the molecular weight of the protein, M_2, according to Equation 24 as illustrated in Figure 2. For proteins which agreggate, the problem becomes complex. Each n-mer aggregate must be treated as a separate solute in deriving the expression for the excess scattering Rayleigh ratio, $\overline{R_\theta}$, from Equation 20. Considering only ideal protein-protein interactions, it can be shown that the y-intercept of the plot of $K(\partial n/\partial c_s)_{T,P,\mu(d)}c_s/\overline{R_\theta}$ versus c_s, where c_s is the total weight concentration of all aggregates, is equal to the inverse of the protein weight-average molecular weight, $M_{w,2}$ (Yamakawa, 1971)

$$M_{w,2} = \frac{\sum_i M_i^2 C_i}{\sum_i M_i C_i} \qquad (25)$$

where the summation is over all protein-aggregate species, at molar concentrations C_i. For this relation to hold, $(\partial n/\partial c_s)_{T,P,\mu(d)}$ must be independent of the aggregate size. If the protein-aggregate size distribution is independent of the protein concentration, a plot of $K(\partial n/\partial c_s)_{T,P,\mu(d)}c_s/\overline{R_\theta}$ versus c_s yields a straight line with a slope related to a z-average of B_{ij}s for all the possible combinations of aggregate species (Yamakawa, 1971).

Usually the protein aggregate size distribution depends on the protein concentration; in that event, the plot is non-linear.

For solutions at low salt concentrations, the preferential-interaction parameter is close to zero and $(\partial n/\partial c_2)_{T,P,\mu(d)}$ can be approximated by $(\partial n/\partial c_2)_{T,P,m}$. For solutions at higher salt concentrations, this approximation breaks down because the salt-protein interactions cannot be ignored. Thus, data can be misinterpretated if $(\partial n/\partial c_2)_{T,P,m}$ is employed instead of $(\partial n/\partial c_2)_{T,P,\mu(d)}$. A plot of $K(\partial n/\partial c_2)_{T,P,m} c_2 / \overline{R_\theta}$ versus c_2 can be fitted to a line provided the protein is not aggregated in solution. The line is given by Equation 22. The slope of this line gives an apparent second virial coefficient, $B_{22,app}$, related to B_{22} by

$$B_{22,app} = \frac{1}{\Omega^2} B_{22} - \frac{1}{\Omega^2}\left(\frac{\partial m_3}{\partial m_2}\right)_{P,\mu(d)}^{\infty} \overline{V}_3^{\infty} \qquad (26)$$

and the apparent molecular weight, $M_{2,app}$, is given by

$$M_{2,app} = \frac{M_2}{\Omega^2} \qquad (27)$$

where Ω is given by Equation 23. If the molecular weight is known, the preferential-interaction parameter can be calculated using Equation 27 and Equation 23 and B_{22} can be evaluated correctly from Equation 26. Thus, B_{22} and $(\partial m_3/\partial m_2)_{T,\mu(d)}$ can be evaluated directly from LALLS data and a value of $(\partial n/\partial c_2)_{T,P,m}$, provided that the molecular weight of the protein is known; in that event, there is no need to determine $(\partial n/\partial c_2)_{T,P,\mu(d)}$. If the protein aggregates, an expression similar to Equation 27 is obtained with M_2 replaced by $M_{w,2}$ under the assumption that the refractive-index increment and the preferential-interaction parameter are independent of aggregate size.

As before, the apparent osmotic second virial coefficient for the aggregated system is related to a z-average of the B_{ij}s.

Experimental Methods

LALLS data and differential refractometry data were obtained for lysozyme and ovalbumin. Lysozyme from chicken egg-white (cat# L-6876) and chicken-egg albumin (ovalbumin, cat# A-5503) were purchased from Sigma Chemical company. Sodium chloride (cat# S271-500), sodium acetate trihydrate (cat# S209-500), ammonium sulfate (cat# A702-500), and sodium phosphate dibasic (cat# S373-500) were purchased from Fisher Scientific company. Sodium sulfate was purchased from J.T. Baker Chemical Co.. Water used to prepare the protein solutions was filtered through a Barnstead-Nanopure Water Purification System.

A Sargent-Welch Model 8400 ion/pH meter with a Fisher Scientific model SN9030116 electrode was used to measure the pH of all solutions. The pH of the salt solutions was adjusted using the strong acid or base of the salt. A bulk dilute protein solution of 100 mL with a concentration between 3 and 5 g/L was prepared by gentle dissolution of the protein in the salt solution. The strong acid or base of the salt at the same ionic strength as the protein solution was used to adjust the pH if there was a change upon dissolving the protein. If there was any sign of irreversible precipitation, the protein solutions were centrifuged at 20,000 rpm, at 20°C, for 20 minutes and the supernatant was removed by gentle pipeting. Five 25 mL protein samples were prepared by diluting the 3-5 g/L protein solution with the salt solution in the following ratios (protein:salt): 1:4, 2:3, 3:2, 4:1, 5:0. Concentrations were measured using a Milton Roy Spectronic 1201 spectrophotometer. A value of 2.63 (cm^2/g) (Sophianopoulus et al., 1962) was used as the extintion coefficient for lysozyme and for ovalbumin, the value used was 0.734 (cm^2/g) (Cunningham and Nueke, 1959).

Light-scattering measurements were performed using an LDC Milton Roy KMX-6 Low Angle Laser Light Scattering (LALLS) photometer which employs a 2mW helium-neon laser at a fixed wavelength 633 nm. For each experiment, the five protein samples and the solvent were filtered through a 0.1um-Millipore filter before analysis. A Sage-Instruments syringe pump was used to pump the samples through the light scattering cell at a rate of 0.3 mL/minute. The scattered light was measured at an angle of 6 to 7 degrees. The Rayleigh ratio is related to the intensity of the scattered light, G_θ, by (LDC/Milton Roy KMX 6 Instruction Manual, 1986)

$$R_\theta = \frac{G_\theta}{G_o}(D)(\sigma' l')^{-1} \tag{28}$$

where D is equal to the transmittance of the attenuators used in measuring the incident light beam, G_o is the intensity of the incident beam passing through the sample cell, and the product $(\sigma' l')^{-1}$ is a geometric term which is a function of the solution refractive-index, field stops, and cell type. Since the calibration method is based on geometry, the resulting measurements are absolute rather than referenced to a known standard.

The difference in refractive-index between the sample and the solvent (Δn) was measured by using an LDC Milton Roy KMX-16 Laser Differential Refractometer which uses a 0.5 mW helium-neon laser at a fixed wavelenth 633 nm. The refractive-index increment at constant salt molality for the protein was determined by plotting $\Delta n/c_2$ for each sample versus its concentration and extrapolating the line to zero protein concentration.

$$\left(\frac{\partial n}{\partial c_2}\right)_{c_2=0,T,m} = \lim_{c_2 \to 0}\left(\frac{\Delta n}{c_2}\right) \tag{29}$$

Refractive-index increments for the protein at constant chemical potentials of water and salt were also measured. To obtain constant chemical potentials of salt and water between the solvent and the protein solution, the protein solutions were dialyzed overnight in 2 L of salt solution at 4°C using a Spectraphor dialysis membrane with a molecular weight cutoff of 5000 to 8000 daltons. The differences in refractive indices between the dialyzates and the respective protein samples were measured. The refractive-index increment for the protein at constant solvent chemical potential was determined by extrapolating the plot of $\Delta n/c_2$ versus concentration to zero.

Data Analysis

B_{22} is related to the overall two-body intermolecular potential by Equation 8, where the potential expression used is given by Equation 9. Figure 3 shows the individual contributions of the potential. The accuracy of the potential expressions can thus be evaluated by comparing experimental B_{22}s with those calculated using Equation 8 and observing agreement with trends of B_{22} with ionic strength and pH. At the experimental salt concentrations employed (1 to 5 molar), contributions from the coulombic-repulsion potential are small due to ionic screening and thus the pH dependence of B_{22} is expected to be small. The ionic-strength dependence of B_{22} is determined mainly by the osmotic-attraction potential since, to a good approximation, the dispersion potential is independent of salt concentration. To evaluate the coulombic-repulsion interaction, the net charge of the protein must be known. The values used here were obtained from a titration of lysozyme in 1 M potasium chloride (Fergg et al., 1994) and the values for ovalbumin were taken from the literature where the titration was also performed in 1 M potassium chloride (Cohn, 1943). Results are shown in Table 1. The titration curve is a function of the salt molality and the type of salt. In general, the addition of salt tends to decrease the activity coefficient of the charged residues by screening intramolecular electrostatic repulsions. This tends to stabilize the more highly

charged species of the protein (Cohn, 1943). Thus, at a given pH, the net charge of the protein is greater at high salt concentrations than that at low salt concentrations. In addition to this effect, the titration curve also depends on the extent of specific ion binding. Binding of cations tends to decrease the pH where the protein has a given positive charge, while binding of anions increases the pH at which the protein has a given negative charge (Fraije and Lyklema, 1991). This effect is most pronounced in salt solutions of low lyotropic-series salts due to their enhanced binding affinities. These effects are ignored in our calculations, since small changes in net charge of the protein do not influence the B_{22} calculation significantly.

Since the proteins are modeled as spheres, an effective spherical radius is calculated from crystal structure dimensions for lysozyme (45x30x30 Å) (Blake et al., 1965) and ovalbumin (70x45x50 Å) (Stein et al., 1990) giving radii 17.2 and 25 Å, respectively. Calculation of the excluded volume of the protein contribution to B_{22} takes into account an impenetratable layer of water surrounding the protein whose size is assumed to be independent of ionic strength and pH. The thickness of the water layer determines the lower limit of integration for the two-body potentials in the B_{22} calculation. Since the two-body potentials are strongest at smallest separations, changing the distance of closest approach can significantly affect the B_{22} calculation. From measurements of the radius of hydration of lysozyme using dynamic light scattering (Rämsch et al., 1995), the thickness of the water layer was estimated to be 1 Ångstrom. By modeling the proteins as spheres, the excluded-volume potential is underestimated because, for a given volume, the excluded-volume potential is a minimum for spheres (Neal and Lenhoff, 1995).

The excluded-volume potential of the salt is determined by the volume of the hydrated salt ion. The size of the hydration layer and the strength of the interaction between water and the ions is related to the ion's position in the lyotropic series. Kosmotropic salts have a high charge density and bind to water strongly, forming a large

hydration layer. On the other hand, the interaction between chaotropic salts and water is weaker than the water-water interaction itself, and the hydration layer is small. The tendency of chaotropes to increase the hydrodynamic radii of nearby solutes is referred to as negative hydration (Collins and Washabaugh, 1985). The sizes of hydrated ionic radii can be calculated from diffusivity, compressibility, conductivity, solubility, and spectroscopic measurements of electrolyte solutions (Amis, 1975; Saluja, 1976). However, the results are rarely in agreement and the choice of hydrated-ion sizes is arbitrary. Unfortunately, the B_{22} calculation is sensitive to the size of the ion because the diameter of the hydrated ion determines the range over which the osmotic force is integrated to obtain B_{22}. This effect is illustrated by Figure 4 which shows B_{22}s calculated for ovalbumin using the DLVO model plus the osmotic-attraction potential with a value of the mean hydrated radius (2.2 Å) and a value of the mean dehydrated (crystal) radius (1.6 Å) for ammonium sulfate. This difference reflects the strong dehydration effect of ammonium sulfate. The values employed here are from Marcus (1993), who calculated the size of the hydration layer based solely on the ion's size and charge.

Since values for the Hamaker constant are known only approximately, on the order of 3-5 kT for most proteins (Nir, 1976), we have chosen to regress values from our data from fitting the experimental B_{22}s. For a moderate pH and ionic-strength range, the Hamaker constant should not change significantly and a constant value indicates that the potential-of-mean-force model is adequate in predicting the solution behavior of the protein.

Experimental Osmotic Virial Coefficients and Interaction Parameters

Tables (2 to 5) present results of the light-scattering and differential-refractometry experiments for lysozyme and ovalbumin in various salt solutions. The apparent weight-average molecular weight, $M_{2,app}$, was calculated from the inverse of the y-intercept of

the light-scattering data according to Equation 22. $M_{2,app}$ is related to the true weight-average molecular weight, $M_{w,2}$, by Equation 27. Shown are the refractive-index increments at constant salt molality, $(\partial n/\partial c_2)_{T,P,m}$, and at constant solvent chemical potential, $(\partial n/\partial c_2)_{T,P,\mu(d)}$. The refractive-index increments at constant chemical potential were either measured experimentally or regressed from LALLS data by fitting $M_{w,2}$ when known. All B_{22} listed were calculated using the regressed refractive-index increments at constant solvent chemical potential because a complete data set for experimental values of $(\partial n/\partial c_2)_{T,P,\mu(d)}$ was not obtained. However, in the cases where $(\partial n/\partial c_2)_{T,P,\mu(d)}$ was measured experimentally, there was good agreement with the regressed values. The preferential-interaction parameter, $(\partial m_3/\partial m_2)_{T,\mu(d)}$, was calculated according to Equation 23 using the regressed values of $(\partial n/\partial c_2)_{T,P,\mu(d)}$. The Hamaker constants were regressed according to Equation 8 as discussed in the *Data Analysis* Section.

For ovalbumin, B_{22} is independent of pH at an ionic strength of 1.0 molar. This is expected from the potential-of-mean-force model (Equation 9) because the only pH-dependent potential is due to coulombic repulsion which is essentially screened out at ionic strength 0.1 molar. B_{22} decreases as the salt concentration rises due to the excluded-volume potential of the salt ions as predicted from the osmotic-attraction potential. The model predicts the ionic-strength dependence well as shown in Figure 5, where experimental and calculated B_{22} (employing a reduced Hamaker constant of 4) are plotted against ionic strength. The regressed Hamaker constants are within the expected range for proteins.

Figure 6 shows the differences in the apparent and true weight-average molecular weights of ovalbumin obtained from light-scattering data. The monomer molecular weight is obtained using the refractive-index increment at constant solvent chemical potential (Equation 24), indicating that no ovalbumin aggregates are present. In contrast, the apparent molecular weights obtained using the refractive-index increment at constant

molality (see Equations 22 and 27) are smaller because the preferential-interaction parameters are significantly negative, reflecting the preferential exclusion of the salt around the protein. The preferential-interaction parameter is independent of pH at 1.0 molar ionic strength and becomes more negative as the ionic strength rises.

Experiments with lysozyme were performed in solutions of ammonium sulfate, potassium sulfate, sodium sulfate, and sodium chloride. Results are listed in Tables 3 through 5. Figure 7 shows the apparent and true weight-average molecular weights obtained for lysozyme in sodium-chloride solutions. The experimental weight-average molecular weight, 17,500 g/mol with sodium chloride, is in excess of the monomer molecular weight, indicating aggregates in solution, consistent with results reported by Haynes et al. (1993) who found weight-average molecular weights between 17,800 and 18,100 g/mol for the same commercial lysozyme with a variety of salts and a range of pH. Although the calculated molecular weights were determined using the refractive-index increment at constant molality, all the experiments were performed at low ionic-strength conditions where the preferential-interaction parameter is small and the weight-average molecular weight obtained using Equation 22 is the same as that of Equation 24. More recently, Skouri et al. (1995) reported that the same commercial lysozyme from Sigma contains 2% ovalbumin and conalbumin which interact with the lysozyme to form large aggregates in aqueous solutions.

Since experimental values of $(\partial n/\partial c_2)_{T,P,\mu(d)}$ were only obtained for the lysozyme experiments in sodium chloride, calculations for the preferential-interaction parameter and B_{22} for lysozyme in the remaining salts were performed using a regressed value for $(\partial n/\partial c_2)_{T,P,\mu(d)}$ from fitting a weight-average molecular weight of 17,800 g/mol. Thus, the state of the lysozyme/ovalbumin aggregation is assumed to be independent of experimental salt conditions. This assumption is important because, to analyze the trends in B_{22} versus pH, ionic strength, and salt type, the state of aggregation must not change as discussed in the *Data Analysis* Section.

Experimental B_{22} values for lysozyme depend on pH for all salt conditions investigated. In general, as pH rises, experimental B_{22}s decrease (see Figure 8), indicating that there is a net gain in attraction at higher pHs. Since electrostatic interactions are effectively screened out at these salt concentrations, the potential-of-mean-force model has no pH dependence and fails to describe this trend. Thus the Hamaker constants regressed depend on pH due to the inability of the model to account for the additional attraction as pH rises. All regressed Hamaker constants are greater than the expected value of 3-5 kT. However, because contributions of the aggregate interactions to the experimental B_{22}s have been ignored, significant error in the Hamaker constant regressions arise if the aggregate interactions are non-ideal (i.e. for an ideal interaction, B_{ij} is equal to zero). Including the effect of aggregation in the regression would be difficult because the experimental B_{22} is a function of the distribution of the aggregate sizes and all possible two-body interactions between the different-sized aggregates. Fortunately, our main concern is the trend in the Hamaker constant with varying solution conditions; its absolute value is not of great importance.

For lysozyme in ammonium sulfate, B_{22} decreases as the salt concentration rises, as expected. There are no trends of the Hamaker constant with ionic strength. For the experiments with lysozyme in sodium chloride, since the Hamaker constants decrease with rising ionic strength, the potential-of-mean-force model overestimates the salt-induced attraction. This error is probably due to overpredicted values for the mean hydrated radius of sodium chloride, as discussed in *Data Analysis* .

The results show that there is a small effect due to the salt type. At pH between 4 and 4.5, the magnitude of B_{22} is significantly less for the sodium sulfate and sodium chloride solutions than for the corresponding ionic-strength solutions of ammonium sulfate. The effect of the salt type is included in the model only in the size of the hydrated ion through the osmotic-attraction potential. Since the sizes of the hydrated radii are similar for all three salts, the differences in the experimental B_{22} are not

predicted by the model and the regressed Hamaker constants are greater for the sodium sulfate and sodium chloride solutions than for ammonium sulfate solutions at the same ionic strengths. This difference could be due to inaccurate values of the hydrated radii of the salt ions since the magnitude of B_{22} is very sensitive to this parameter, as shown in Figure 4.

Figure 9 shows the preferential-interaction parameter plotted versus pH for ammonium sulfate solutions of lysozyme. For all experiments in ammonium sulfate, preferential exclusion of the salt around the protein increases as pH rises, probably because there is specific ion binding of the sulfate ion to the positively charged residues of lysozyme at the lower pHs.

Discussion

Light-scattering data for ovalbumin and lysozyme show that the potential-of-mean-force model is adequate for describing solution behavior at moderate to high ionic strengths. Salt-induced attraction is a result of the excluded-volume potential of the salt which is either magnified or reduced, depending on the nature of the salt-water interaction. Since the salts used here interact strongly with water, their hydrated size is larger, resulting in longer-ranged osmotic forces. The kosmotropic nature of the salts employed is supported by the observation that they are preferentially excluded around the protein.

B_{22} depends on salt type for lysozyme, which is not predicted by the current model, although model results could be corrected by adjusting the sizes of the hydrated salt ions. However, the effect of salt on hydrophobic interactions may be a factor in determining protein-protein interactions at high salt concentration. It has been shown that the strength of the hydrophobic interaction between two hydrophobic surfaces is ten times as strong as the dispersion interaction and has the same distance dependence (Israelachvilli and Pashley, 1982). Thus, this interaction is significant for proteins that

have a considerable number of exposed apolar residues. Since hydrophobic interactions are not taken into account by the model, the Hamaker constant must depend on the hydrophobicity of the molecule. Since it has been shown that kosmotropic salts enhance hydrophobic interactions, it is possible that the addition of kosmotropic salt can significantly increase the protein-protein attraction by strengthening the hydrophobic interactions, resulting in a more attractive B_{22} for high lyotropic-series salts.

The pH trend of the experimental B_{22} for lysozyme in ammonium sulfate cannot be explained by the potential-of-mean-force model because it does not predict any pH dependence at high salt concentrations. Experiments performed with lysozyme at low ionic strength have shown that lysozyme aggregates in an isodesmic head-to-tail manner if the pH is above 4.5 (Banerjee et al., 1975; Brusezzi et al., 1965). Although this association is not detected under high-salt conditions (Rämsch, 1995), there might still be some residual pH-dependent attraction between the lysozyme molecules which is not strong enough to promote association.

The results for the preferential-interaction parameter for lysozyme in ammonium sulfate indicate that there is an increase in salt exclusion as pH rises. This phenomenon is most likely due to specific ion binding of the sulfate ion to the positively charged residues of lysozyme at low pH. Sulfate binding can explain the observed pH trend of B_{22} in terms of hydration forces. Hydration forces arise whenever water molecules are highly structured or ordered around surface polar groups. The mechanism for the interaction is not fully understood, although the strength of the force has been found to depend on the energy needed to dehydrate the surface (Israelachvili, 1992). This dependence comes from measurements of the forces between negatively charged mica surfaces in dilute electrolyte solutions. At low salt concentrations, no hydration force was observed. However, at the higher salt concentrations, it was found that hydrated cations bind to the mica surfaces, giving rise to repulsive hydration forces (Israelachvili and Pashley, 1982; Pashley, 1982) which are characterized by a short-ranged oscillatory force superimposed

upon an exponentially decaying repulsive force with a range of about 10 Ångstroms (Israelachvili and Pashley, 1983). The strength and range of the interaction is related to the ion's position in the lyotropic series, increasing with rising hydration number in the order $Mg^{+2}>Ca^{+2}>Li^{+}\sim Na^{+}>K^{+}>Cs^{+}$. Israelachvili (1992) showed that these forces can be modified by exchanging ions with different hydrations on surfaces. Thus, at low pH, significant sulfate binding to the negatively charged residues can lead to strong hydration forces because of the strong attractive interaction between the sulfate ion and water.

Figure 10 shows a plot of B_{22} for lysozyme in solutions of sodium chloride and ammonium sulfate versus ion concentration along with the crystallization window proposed by George and Wilson (1994). While crystallization occurs for the solutions of lysozyme and sodium chloride that fall in the crystallization window, addition of ammonium sulfate results in solely amorphous precipitation. Thus the simple concept of a crystallization window needs refinement. Further insight into the conditions that favor crystallization can be gained by determining the individual contributions to the total pair potential. For example, since less salt is required to obtain the same level of attraction between lysozyme molecules in solutions of sodium chloride than in solutions of ammonium sulfate, the attraction due to osmotic forces is a larger fraction of the overall pair potential for solutions of ammonium sulfate. It is possible that the conditions where osmotic forces dominate lead to amorphous precipitation because these forces are centrosymmetric and require no geometrical complimentarity or orientation between the protein molecules. On the other hand, for crystallization, protein molecules need to be orientated with respect to each other so that short-ranged electrostatic (i.e. hydrogen bonds, salt bridges) forces can be effective. It is likely that these types of interactions dominate at conditions favorable for crystallization.

Conclusions

Understanding the factors that affect salt-induced protein phase separation also provides insight into the types of factors that may play a role in determining those solution conditions that are favorable for crystallization or for amorphous precipitation. However, to provide a better understanding of the effect of salt on protein solubility, we need to know if the second virial coefficient provides an accurate measure of the overall specific and noncentrosymmetric forces that stabilize amorphous precipitates and crystals. In other words, we need to understand better the various contributions to the protein-protein second virial coefficient in salt-containing solutions. At the present time, the forces that contribute to B_{22} at high salt concentrations are not sufficiently well understood in terms of simple DLVO theory and the osmotic-attraction potential. Hydration forces and other specific forces probably contribute significantly to the total pair potential at high salt concentrations. These forces must be understood to develop a diagnostic better than the proposed crystallization window of George and Wilson (1994).

Acknowledgements

This work was supported by the National Science Foundation (grant #9214653) and by the Director, Office of Energy Research, Office of Basic Energy Sciences, Chemical Sciences Division of the U.S. Department of Energy under Contract Number DE-AC03-76SF00098.

References

Amis, E.S., "Solvation of Ions," in *Solutions and Solubilities*, Part 1, M.R.J. Dack, ed., Wiley (Interscience), New York and London (1975).

Arakawa, T., Bhat, R., and S.N. Timasheff, "Preferential Interactions Determine Protein Solubility in Three-Component Solutions: $MgCl_2$ System," *Biochemistry*, **29**, 1914 (1990).

Arakawa, T. and S.N. Timasheff, "Theory of Protein Solubility," *Meth. Enzymology*, **114**, 49 (1985).

Arakawa, T. and S.N. Timasheff, "Preferential Interactions of Proteins with Salts in Concentrated Solutions," *Biochemistry*, **21**, 6545 (1982)

Asakura, S., and F. Oosawa, "On Interaction Between Two Bodies Immersed in a Solution of Macromolecules," *J. Chem. Phys.* **22**, 1255 (1954).

Asakura, S., and F. Oosawa, "Interaction Between Particles Suspended in Solutions of Macromolecules," *J. Polym. Sci.*, **33**, 183 (1958).

Banerjee, S.K., A. Pogolotti, and J.A. Rupley, "Self-Association of Lysozyme," *J. Biol. Chem.*, **250**, 8260 (1975).

Baxter, R.J., "Percus-Yevick Equation for Hard Spheres with Surface Adhesion," *J. Chem. Phys.*, **49**, 2770 (1968).

Blake, C.C.F., D.F. Koenig, G.A. Mair, A.C.T. North, D.C. Phillips, and V.R. Sarma, "Structure of Hen Egg-White Lysozyme,"*Nature*, **206**, 757 (1965).

Brusezzi, M.R., E. Chiancone, and E. Antonini, "Association-Dissociation Propeties of Lysozyme," *Biochemistry*, **4**, 1796 (1965).

Casassa, E.F., and H. Eisenberg, "Thermodynamic Analysis of Multicomponent Solutions," *Adv. Protein. Chem.*, **19**, 287 (1964).

Chiew, Y.C., D. Kuehner, H.W. Blanch, and J.M. Prausnitz, "Molecular Thermodynamics for Salt-Induced Protein Preciptation," *AIChE J.*, **41**, 2150 (1995).

Coen, C.J., H.W. Blanch, and J.M. Prausnitz, "Salting-Out of Aqueous Proteins: Phase Equilibria and Intermolecular Potentials," *AIChE J.*, **41**, 996 (1995).

Cohn, E.J., "The Physical Chemistry of Proteins," *Physiol. Rev.*, 5, 349 (1925).

Cohn, E.J., "The Solubility of Proteins," *Proteins, Amino Acids, and Peptides*, E.J. Cohn and J.T. Edsall, ed., Reinhold, New York, chap. 23 (1943).

Collins, K.D. and M.W. Washabaugh, "The Hofmeister Effect and the Behavior of Water at Interfaces," *Q. Rev. Biophys.*, **18**, 323 (1985).

Cunningham, J.C., and B.J. Muenke, "Physical and Chemical Studies of a Limited Reaction of Iodine with Proteins,"*J. Biol. Chem.*, **234**, 1447 (1959).

Fergg, F., D.Kuehner, H.W. Blanch, and J.M. Prausnitz, "Hydrogen Ion Titrations of Amino Acids and Proteins in Solutions Containing Concentrated Electrolyte," Diplomarbeit, Technische Universität München (1994).

Foster, P.R., "Protein Precipitation," in *Engineering Processes for Bioseparations,* L.R. Weatherley, Ed., Butterworth-Heinemann, Oxford, (1994).

George, A., and W.W. Wilson, "Predicting Protein Crystallization from a Dilute Solution Property," *Acta Cryst.*, **D50**, 361 (1994).

Hamaker, H.C., "The London-Van-der Waals Attraction Between Spherical Particles," *Physica IV*, **10**, 1058 (1937).

Haynes, C.A., F.J. Benitez, H.W. Blanch, and J.M. Prausnitz, "Application of Integral-Equation Theory to Aqueous Two-Phase Partitioning Systems," *AIChe J.*, **39**, 1539 (1993).

Hill, T.L., "Theory of Solutions. I," *J. Amer. Chem. Soc.*, **79**, 4885 (1957).

Howell, P.L., "Structure of Hexagonal Turkey Egg-White Lysozyme at 1.65 Å Resolution," *Acta Cryst.*, **D51**, 654 (1995).

Inoue, H., and S.N. Timasheff, "The Interaction of β-Lactoglobulin with Solvent Components in Mixed Water-Organic Solvent Systems," *J. Amer. Chem. Soc.* **90**, 1890 (1968).

Israelachvili, J.N., *Intermolecular and Surface Forces: With Applications to Colloidal and Biological Systems*, 2nd ed., Academic Press, London (1992).

Israelachvili, J.N., and Pashley, R.M., "Double-Layer, Van-der Waals, and Hydration Forces Between Surfaces in Electrolyte Solutions," in *Biophysics of Water*, F. Franks, ed., Wiley, New York, 183 (1982).

Israelachvili, J.N., and Pashley, R.M., "Molecular Layering of Water at Surfaces and Origin of Repulsive Hydration Forces," *Nature*, **306**, 249 (1983).

Jervis, L., W.S. Pierpoint, "Purification Technologies for Plant Proteins," *J. Biotechnol.*, **11**, 161 (1989).

Kirkwood, J.G., "The Theoretical Interpretation of the Properties of Solutions of Dipolar Ions," in *Proteins, Amino Acids, and Peptides*, E.J. Cohn and J.T. Edsall, Ed., Reinhold, New York (1943).

Kirkwood, J.G., and Goldberg, R.J., "Light Scattering Arising from Composition Fluctuations in Multi-Component Systems," *J. Chem. Phys.*, **18**, 54 (1950).

Lambert, P.W. and J.L. Meers, "The Production of Industrial Enzymes," *Phil. Trans. R. Soc. Lond.*, **B300**, 262 (1983).

Lee, C.L., K. Gekko, and S.N. Timasheff, "Measurement of Preferential Solvent Interactions by Densimetric Techniques," *Methods in Enzymology*, **61**, 26 (1979).

Lovrien, R.E., M.J. Conroy, and T.I. Richardson, "Molecular Basis for Protein Separations," in *Protein-Solvent Interactions*, R.B. Gregory, Ed., Marcel Dekker, New York, 521 (1995).

Marcus, Y., "A Simple Empirical Model Describing the Thermodynamics of Hydration of Ions of Widely Varying Charges, Sizes, and Shapes," *Biophys. Chem.*, **51**, 111 (1994).

McMillan, Jr., W.G., and J.E. Mayer, "The Statistical Thermodynamics of Multicomponent Systems,"*J. Chem. Phys.*, **13**, 276 (1945).

Melander, W., and C. Horvath, "Salt Effects on Hydrophobic Interactions in Precipitation and Chromatography of Proteins: An Interpretation of Lyotropic Series," *Arch. Biochem. Biophys.*, **183**, 200 (1977).

McPherson, A., "Current Approaches to Macromolecular Crystallization," *Eur. J. Biochem.*, **189**, 1 (1990).

Neal, B.L., and A.M. Lenhoff, "Excluded Volume Contribution to the Osmotic Second Virial Coefficient for Proteins," *AIChE J.*, **41**, 1010 (1995).

Nir, S. "Van-der Waals Interactions Between Surfaces of Biological Interest," *Prog. Surf. Sci.*, **8**, 1 (1976).

Pashley, R.M., "Hydration Forces Between Mica Surfaces in Electrolyte Solutions," *Adv. Colloid Interface Sci.*, **16**, 57 (1982).

Rämsch, C., D.Kuehner, H.W. Blanch, and J.M. Prausnitz, "Dynamic Light Scattering Studies of Aqueous Protein Solutions Containg Salts," Diplomarbeit Thesis, IVT RWTH-Aachen (1995).

Rosenbaum, D., P.C. Zamora, and C.F. Zukoski, "Phase Behavior of Small Attractive Colloidal Particles," *Phys. Rev. Let.*, **76**, 150 (1996).

Rothstein, F., "Differential Precipitation of Proteins," in *Protein Purification Process Engineering*, R.G. Harrison, Ed., Marcel Dekker, New York, 115 (1994).

Saluja, P.P.S., "Environment of Ions in Aqueous Solutions," *Int. Rev. Sci. Electrochemistry*, **6**, 1 (1976).

Shih, Y-C., J.M. Prausnitz, and H.W. Blanch, "Some Characteristics of Protein Precipitation by Salts," *Biotech. and Bioeng.*, **40**, 1155 (1992).

Sinanoglu, O., "Solvent Effects on Molecular Association," in *Molecular Associations in Biology*, B. Pullman, ed., Academic Press, New York, 427 (1968).

Skouri, M., B. Lorber, R. Giege, J.P. Munch, and J.S. Candau, "Effect of Macromolecular Impurities on Lysozyme Solubility and Crystallizability: Dynamic Light Scattering, Phase Diagram, and Crystal Growth Studies," *J. Cryst. Growth*, **152**, 209 (1995).

Sophianopoulus, A.J., C.K. Rhodes, D.N. Holcomb, and K.E. van Holde, "Physical Studies of Lysozyme,"*J. Biol. Chem.* **237**, 1107 (1962).

Stein, P.E., G.W. Leslie, J.T. Finch, D.J. McLaughlin, and R.W. Carrell, "Crystal Structure of Ovalbumin as a Model for the Reactive Centre of Serpins," *Nature*, **347**, 99 (1990).

Stockmayer, W.H., "Light Scattering in Multi-Component Systems," *J. Chem. Phys.*, **18**, 58 (1950).

Stryker, M.H., M.J. Bertolini, and Y.-L. Hao, "Blood Fractionation: Proteins," in *Advances in Biotechnological Processes, Volume 4,* A. Mizrahi and A.L. van Wezel, Ed., Alan R. Liss, New York, (1985).

Takahashi, T., S. Endo, and K. Nagayama, "Stabilization of Protein Crystals by Electrostatic Interactions as Revealed by a Numerical Approach," *J. Mol. Biol.*, **234**, 421 (1993).

Tanford, C., *Physical Chemistry of of Macromolecules*, John Wiley and Sons, New York (1961).

Timasheff, S.N., T. Arakawa, "Mechanism of Protein Precipitation and Stabilization by Co-Solvents," *J. Cryst. Growth*, **90**, 39 (1988).

Verwey, E.J.W., and J.T.K. Overbeek, *Theory of Stability of Lyophobic Colloids,* Elsevier, Amsterdam (1948).

Vilker, V.L., C.K. Colton, and K.A. Smith, "Osmotic Pressure of Concentrated Protein Solutions: The Effect of Concentration and pH in Saline Solutioons of Bovine Serum Albumin," *J. Colloid Interf. Sci.*, **79**, 548 (1981).

Vlachy, V., H.W. Blanch, and J.M. Prausnitz, "Liquid-Liquid Phase Separations in Aqueous Solutions of Globular Proteins," *AiChE J.*, **39**, 215 (1993).

Vlachy, V., and J.M. Prausnitz, "Donnan Equilibrium. Hypernetted-Chain Study of One-Component and Multicomponent Models for Aqueous Polyelectrolyte Solutions," *J. Phys. Chem.*, **96**, 6465 (1992).

Wilson, W.W., "The Second Virial Coefficient as a Predictor in Protein Crystal Growth," ACS Annual Meeting, New Orleans (1996).

Yamakawa, H., *Modern Theory of Polymer Solutions*, Harper and Row, Publishers, New York, (1971).

Zimmerman, S.B. and A.P. Minton, "Macromolecular Crowding: Biochemical, Biophysical, and Biological Consequences," *Ann. Rev. Biophys. Biomol. Struct.*, **22**, 27 (1993).

Table Captions

Table 1. Electric charge of ovalbumin and lysozyme as a funtion of pH in 1.0 molar potassium chloride.

Table 2. LALLS and differential-refractometry measurements of ovalbumin in ammonium-sulfate solutions at 25°C. 2 - protein, 3 - salt.

Table 3. LALLS and differential-refractometry measurements of lysozyme in sodium-chloride solutions with 50-mM sodium acetate buffer, pH 4.5 at 25°C. 2 - protein, 3 - salt.

Table 4. LALLS and differential-refractometry measurements for lysozyme in ammonium-sulfate solutions at 25°C. 2 - protein, 3 - salt.

Table 5. LALLS and differential-refractometry measurements of lysozyme in potassium-sulfate and sodium-sulfate solutions at 25°C. 2 - protein, 3 - salt.

Figure Captions

Figure 1. Contributions to the Gibbs energy (a) and total Gibbs energy (b) of transferring a protein from salt-free water to a salt solution as a function of salt molality m_3.

Figure 2. Light-scattering data for lysozyme in 1.0 molar ionic-strength ammonium sulfate at pH 5.

Figure 3. Intermolecular potentials for lysozyme in 1.0 M NaCl at a pH of 4.5 for a Hamaker constant of 5 kT and a mean salt diameter of 4.4 Å.

Figure 4. B_{22} calculated using the DLVO model and the osmotic attraction potential with a hydrated radius of 2.2 Å and a dehydrated radius of 1.6 Å for the salt ions for ovalbumin in ammonium sulfate solutions versus ionic strength at pH 6.

Figure 5. Experimental and calculated values of B_{22} (H=4kT), based on the DLVO model and osmotic attraction potential, versus ionic strength for ovalbumin in ammonium sulfate solutions of pH 6.

Figure 6. Molecular weights calculated using $(dn/dc_2)_m$ and $(dn/dc_2)_\mu$ versus ionic strength for ovalbumin in ammonium-sulfate solutions at pH 6.

Figure 7. Molecular weights obtained using $(dn/dc_2)_m$ and $(dn/dc_2)_\mu$ versus ionic strength for lysozyme in sodium-chloride solutions at pH 4.5.

Figure 8. B_{22} versus pH for lysozyme in solutions of ammonium sulfate at different ionic strengths.

Figure 9. The preferential interaction parameter versus pH for lysozyme in ammonium sulfate solutions.

Figure 10. B_{22} versus ion concentration for lysozyme in solutions of sodium chloride and ammonium sulfate. The position of the crystallization window is shown. Protein solutions in sodium chloride yield crystals, while those in solutions of ammonium sulfate lead to amorphous precipitation.

pH	4	5	6	7	8	9
ovalbumin	20	-2	-8	-12	-14	-16
lysozyme	14	11	9	8	7.5	7

Table 1

Ionic Strength, pH (molar)	$(\partial n/\partial c_2)_m$ (mL/g)	$M_{2,app}$ (g/mol)	experimental $(\partial n/\partial c_2)_\mu$ (mL/g)	regressed $(\partial n/\partial c_2)_\mu$ (mL/g)	$B_{22} \times 10^4$ (mLmol/g^2)	regressed H/kT	$(\partial m_3/\partial m_2)_{\mu(d)}$ mol/mol
1, 5	0.191	40,000		0.183	-1	5	-17
1, 6	0.191	41,000	0.183	0.185	-0.2	3	-15
1, 7	0.189	41,000		0.182	0	3.6	-15
1, 8	0.194	40,000		0.184	0.4	2.6	-21
3, 6	0.182	36,000	0.169	0.165	-0.5	2.9	-37
4, 6			0.145	0.153	-1.3	3	
5, 6	0.161	36,000		0.145	-4.1	3.8	-39
7, 6				0.127	-16	4.4	

Table 2

Ionic Strength (molar)	$(\partial n/\partial c_2)_m$ (mL/g)	$M_{2,app}$ (g/mol)	experimental $(\partial n/\partial c_2)_\mu$ (mL/g)	regressed $(\partial n/\partial c_2)_\mu$ (mL/g)	$B_{22} \times 10^4$ (mLmol/g^2)	regressed H/kT	$(\partial m_3/\partial m_2)_{\mu(d)}$ mol/mol
0.171	0.182	17,200		0.179	1	9.8	-4
0.342	0.181	17,000	0.179	0.177	-3	10.7	-5
0.684	0.179	17,000	0.176	0.175	-4.3	9.6	-5
1.03	0.175	16,600	0.17	0.169	-5.6	9.1	-8
1.37				0.166	-6	8.4	
1.71	0.171	16,600		0.165	-8.4	8.5	-8

Table 3

Ionic Strength, pH (molar)	$(\partial n/\partial c_2)_m$ (mL/g)	regressed $(\partial n/\partial c_2)_\mu$ (mL/g)	$M_{2,app}$ (g/mol)	$B_{22} \times 10^4$ (mLmol/g^2)	regressed H/kT	$(\partial m_3/\partial m_2)_{\mu(d)}$ mol/mol
1, 4	0.175	0.17	16,800	0.1	6.2	-3
1, 5	0.171	0.165	16,600	-2.8	8.3	-4
1, 7	0.181	0.168	15,300	-5.3	9.1	-9
3, 4	0.159	0.151	16,200	-4.1	6.7	-6
3, 7	0.163	0.152	15,500	-6.1	7.6	-8
3, 8		0.151		-7.6	8.2	
5, 4	0.147	0.139	15,900	-15	7.9	-6
5, 5	0.154	0.142	15,000	-11.2	7	-9
5, 7	0.156	0.141	14,500	-16.7	8.2	-11
5, 8	0.157	0.138	13,800	-17.1	8.2	-14

Table 4

Ionic Strength, pH (molar)	$(\partial n/\partial c_2)_m$ (mL/g)	regressed $(\partial n/\partial c_2)_\mu$ (mL/g)	$M_{2,app}$ (g/mol)	$B_{22} \times 10^4$ (mLmol/g^2)	regressed H/kT	$(\partial m_3/\partial m_2)_{\mu(d)}$ mol/mol
1 K_2SO_4, 7	0.179	0.167	15,500	-4.8	9.1	-8
1 K_2SO_4, 9	0.171	0.165	16,400	-6	9.6	-5
3 Na_2SO_4, 4	0.155	0.151	16,900	-8	8	-3
3 Na_2SO_4, 7	0.167	0.153	14,700	-10.3	8.7	-9
3 Na_2SO_4, 9	0.161	0.152	15,700	-12.5	9.2	-6

Table 5

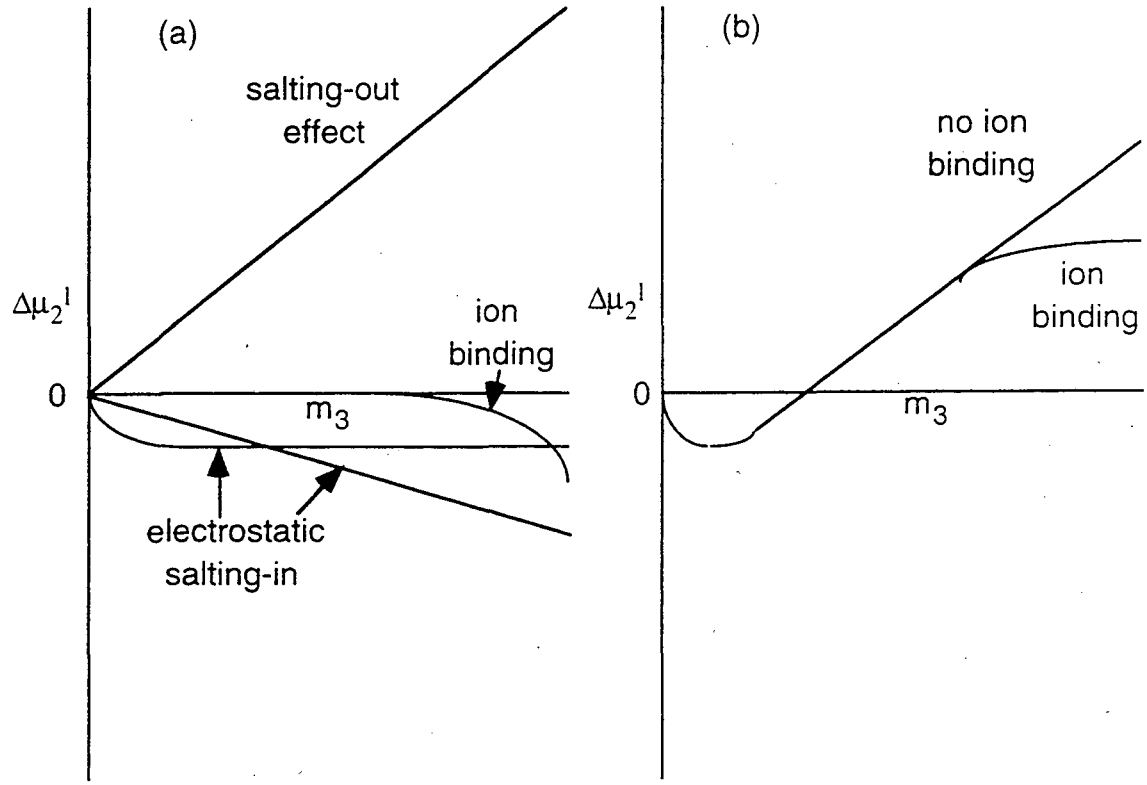
(a)
salting-out
effect
$\Delta\mu_2^I$
ion
binding
0
m_3
electrostatic
salting-in
(b)
no ion
binding
ion
binding
$\Delta\mu_2^I$
0
m_3

Figure 1

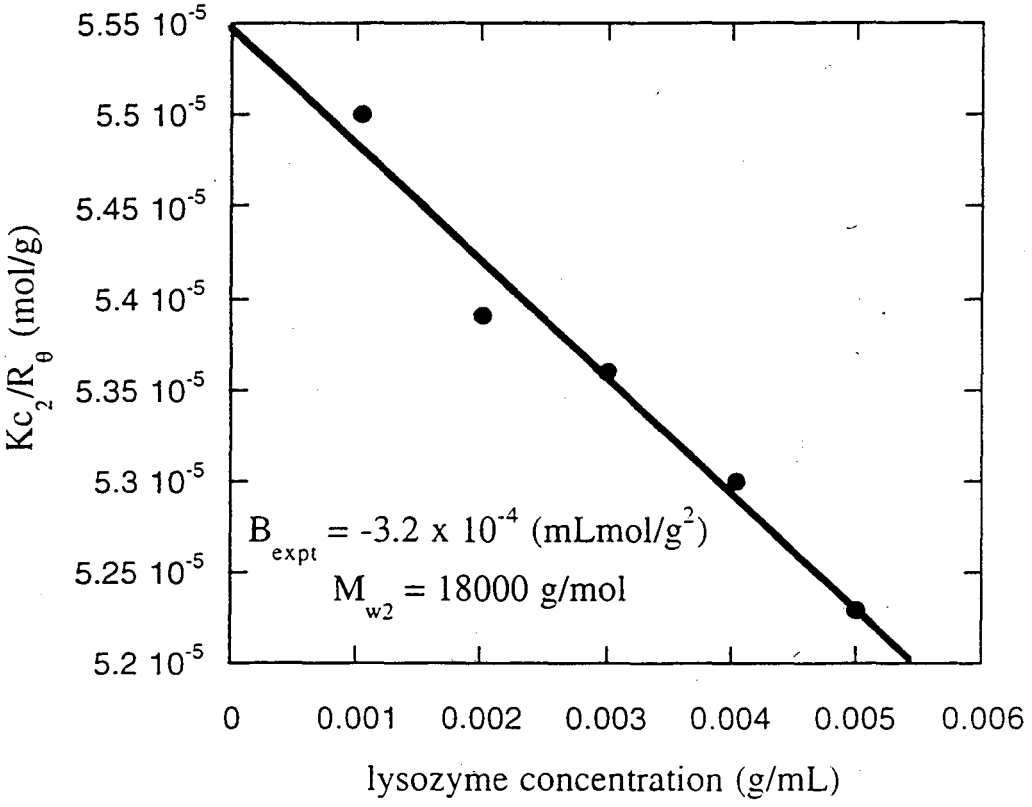
5.55 10-5
5.5 10-5
5.45 10-5
5.4 10-5
5.35 10-5
5.3 10-5
5.25 10-5
5.2 10-5
Kc2/Rθ (mol/g)
Bexpt = -3.2 x 10-4 (mLmol/g2)
Mw2 = 18000 g/mol
0
0.001
0.002
0.003
0.004
0.005
0.006
lysozyme concentration (g/mL)

Figure 2

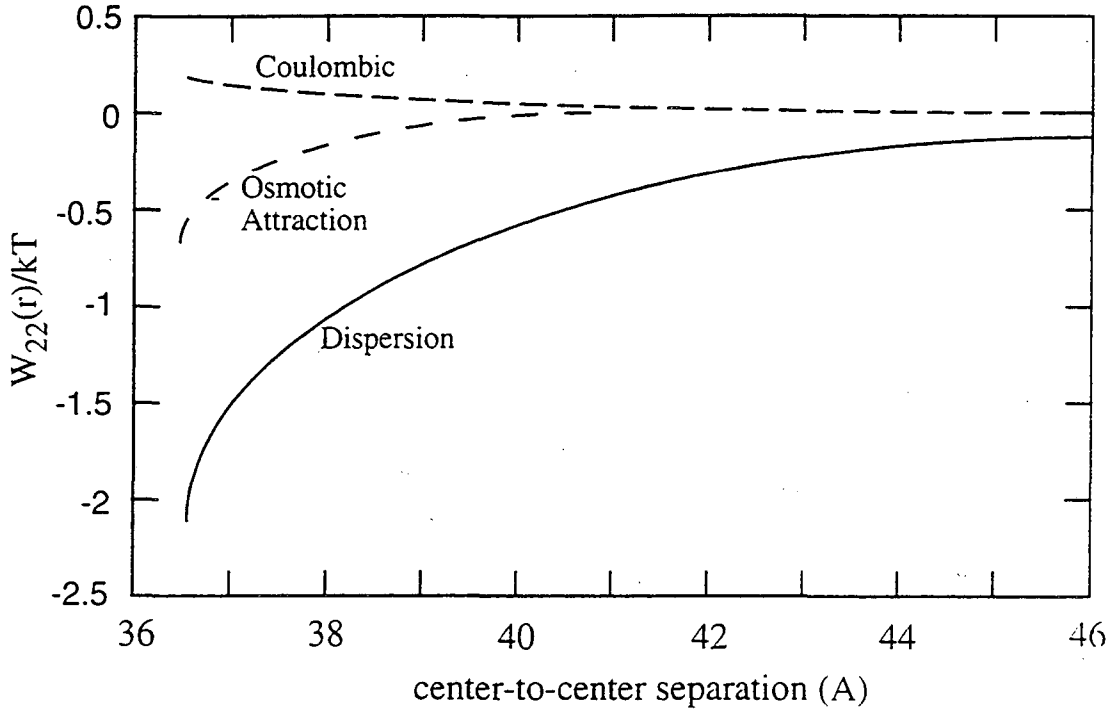
0.5
0
-0.5
-1
-1.5
-2
-2.5
$W_{22}(r)/kT$
Coulombic
Osmotic
Attraction
Dispersion
36
38
40
42
44
46
center-to-center separation (A)

Figure 3

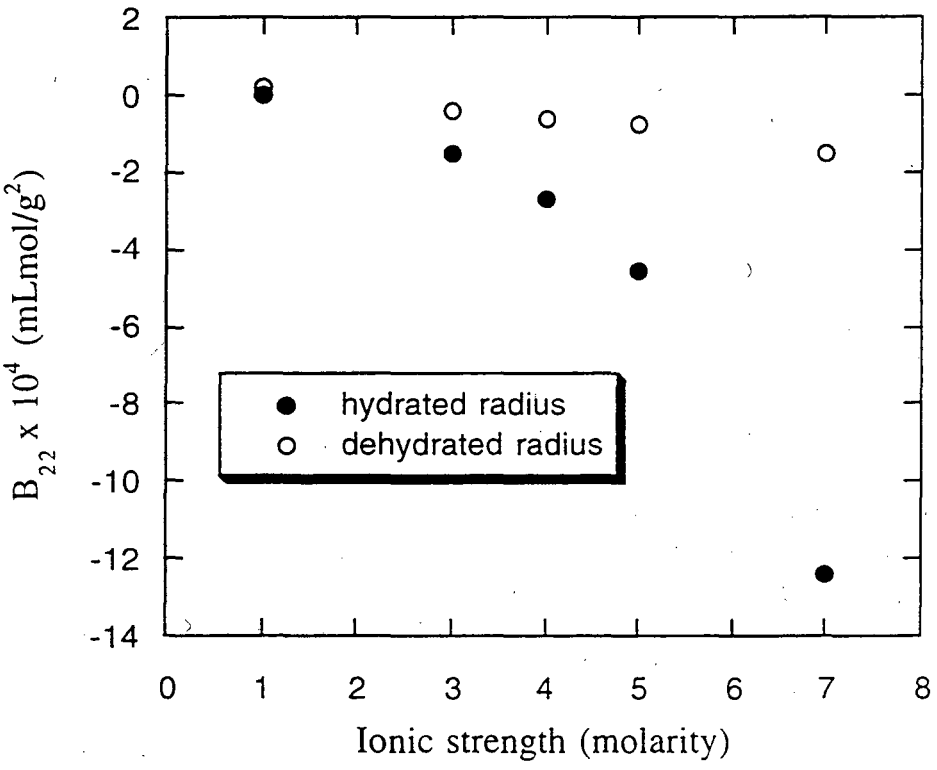
2
0
-2
-4
-6
-8
-10
-12
-14
B_{22} x 10^4 (mLmol/g^2)
hydrated radius
dehydrated radius
0
1
2
3
4
5
6
7
8
Ionic strength (molarity)

Figure 4

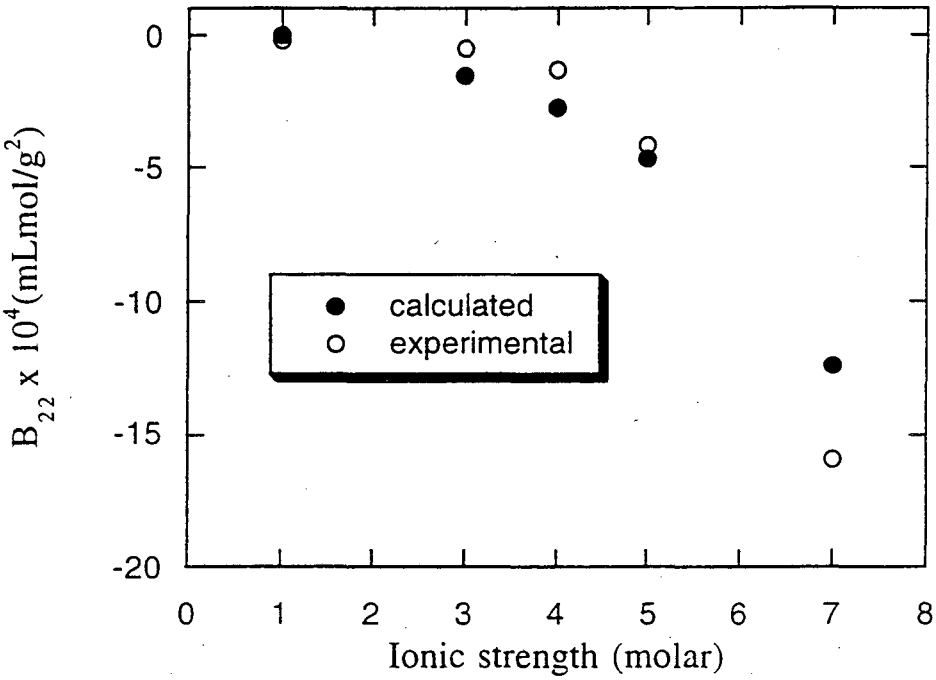
0
-5
-10
-15
-20
0
1
2
3
4
5
6
7
8
B_{22} x 10^4(mLmol/g^2)
Ionic strength (molar)
calculated
experimental

Figure 5

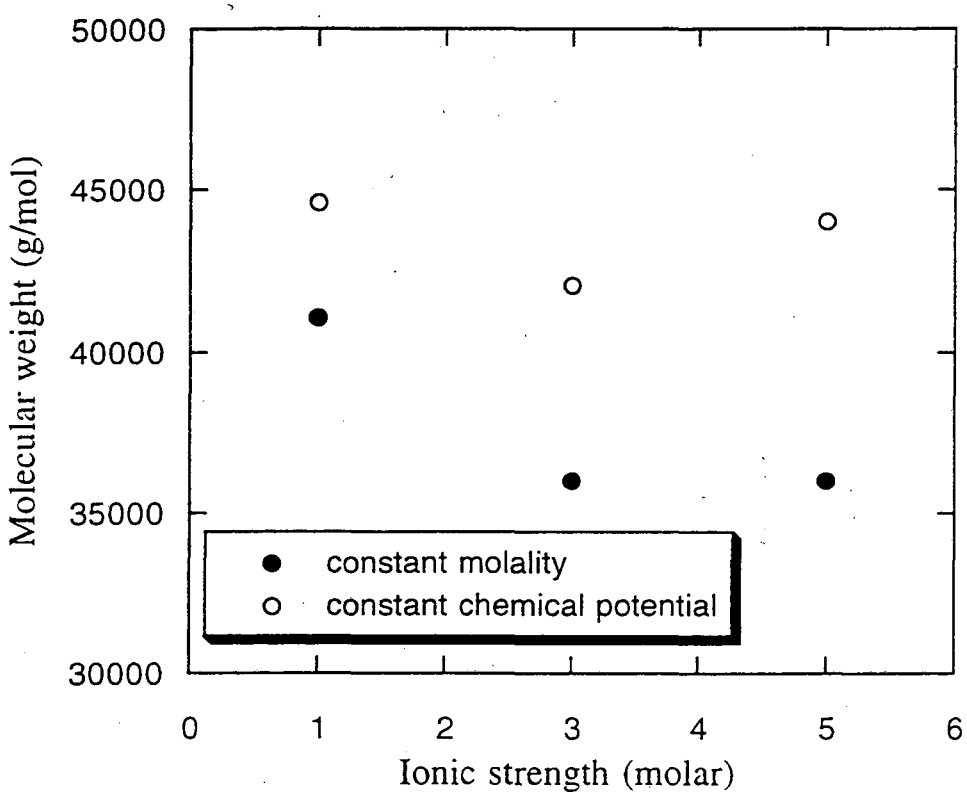
50000
45000
40000
35000
30000
Molecular weight (g/mol)
0
1
2
3
4
5
6
Ionic strength (molar)
constant molality
constant chemical potential

Figure 6

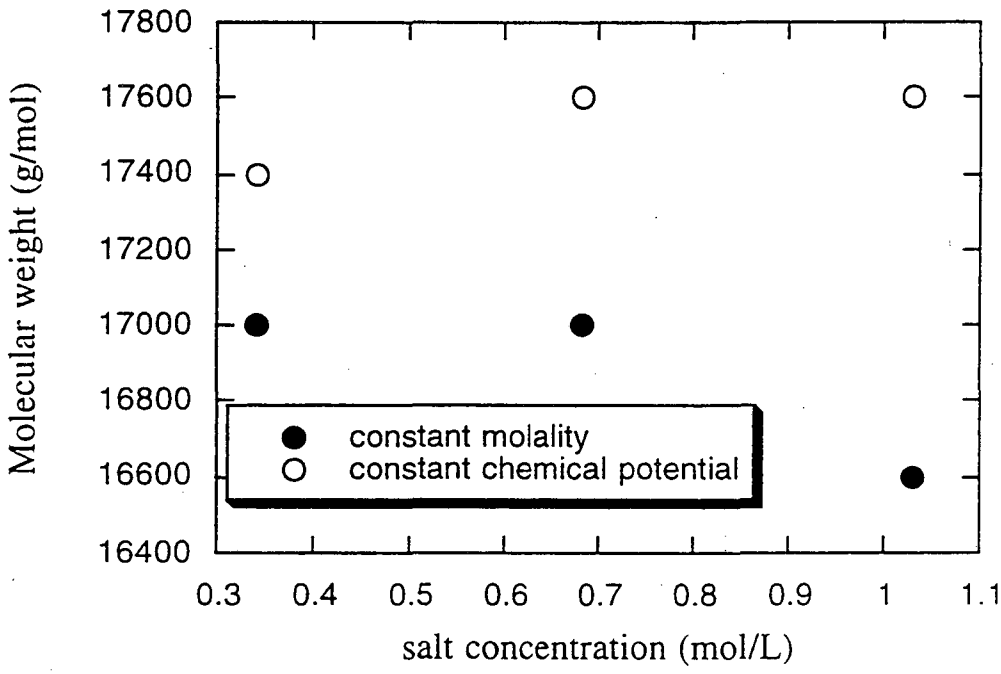
Molecular weight (g/mol)
17800
17600
17400
17200
17000
16800
16600
16400
0.3
0.4
0.5
0.6
0.7
0.8
0.9
1
1.1
salt concentration (mol/L)
constant molality
constant chemical potential

Figure 7

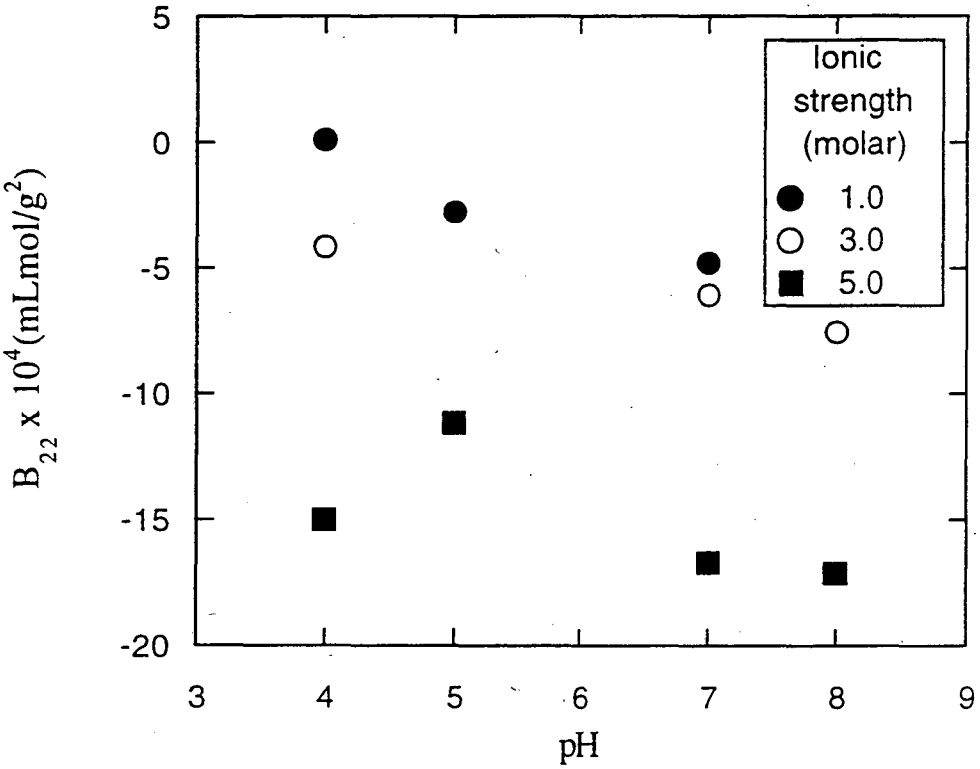
5
0
-5
-10
-15
-20
3
4
5
6
7
8
9
pH
B_{22} x 10^4(mLmol/g^2)
Ionic strength (molar)
1.0
3.0
5.0

Figure 8

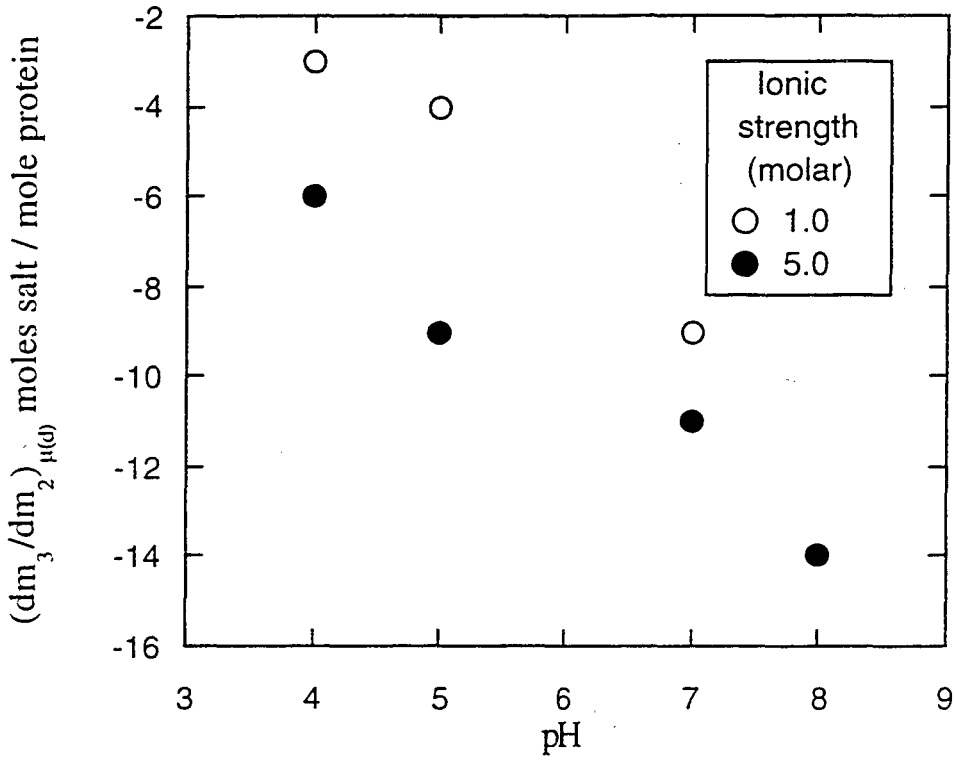
-2
-4
-6
-8
-10
-12
-14
-16
3
4
5
6
7
8
9
pH
$(dm_3/dm_2)_{\mu(d)}$ moles salt / mole protein
Ionic strength (molar)
1.0
5.0

Figure 9

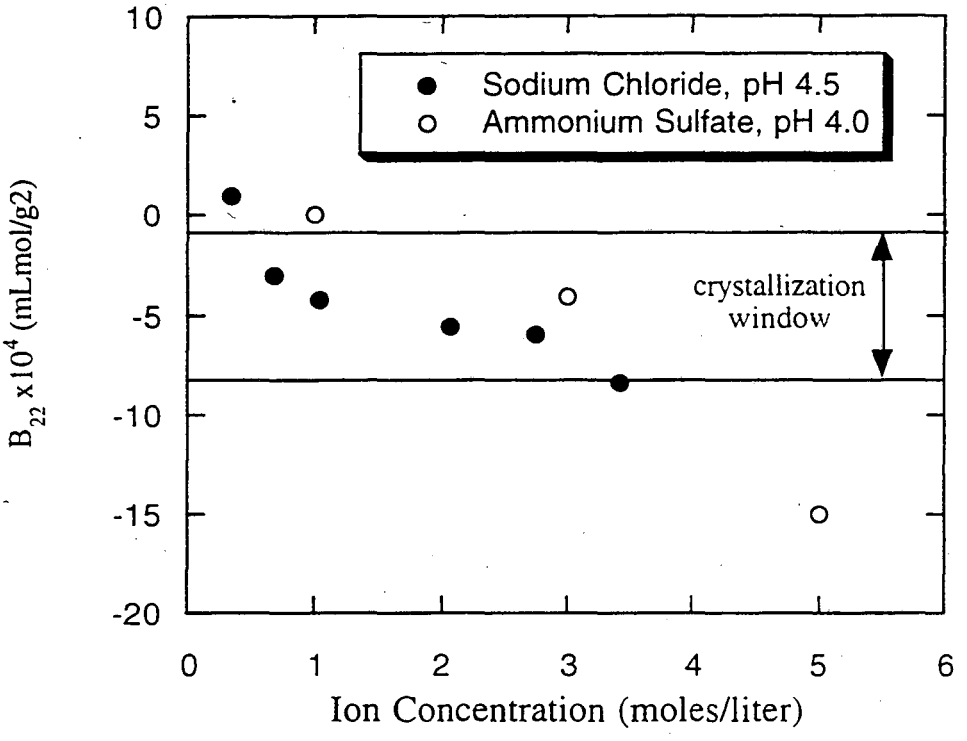
Sodium Chloride, pH 4.5
Ammonium Sulfate, pH 4.0
crystallization window
B_{22} x10^4 (mLmol/g2)
Ion Concentration (moles/liter)
10
5
0
-5
-10
-15
-20
0
1
2
3
4
5
6

Figure 10

Ernest Orlando Lawrence Berkeley National Laboratory
One Cyclotron Road | Berkeley, California 94720

Prepared for the U.S. Department of Energy under Contract No. DE-AC03-76SF00098